coatings

MDPI

Article

Cinnamon Essential-Oil-Loaded Fish Gelatin–Cellulose Nanocrystal Films Prepared under Acidic Conditions

Abdollah Golmohammadi [1,*], Mahsa Sadat Razavi [1], Mohammad Tahmasebi [1], Daniele Carullo [2] and Stefano Farris [2,*]

[1] Department of Biosystem Engineering, University of Mohaghegh Ardabili, Daneshgah Street, Ardabil 56199-11367, Iran; mahsarazavi.68@gmail.com (M.S.R.); m.tahmasebi@uma.ac.ir (M.T.)
[2] Food Packaging Laboratory, Department of Food, Environmental and Nutritional Sciences (DeFENS), University of Milan, Via Celoria 2, 20133 Milan, Italy; daniele.carullo@unimi.it
* Correspondence: golmohammdi1342@gmail.com (A.G.); stefano.farris@unimi.it (S.F.); Tel.: +98-045-1551-7500 (A.G.); +39-02-5031-6805 (S.F.); Fax: +98-045-1552-0567 (A.G.); +39-02-5031-6672 (S.F.)

Abstract: The aim of this study was to characterize films obtained from fish gelatin (GelA, 3% *w*/*w*), encapsulated with cinnamon essential oil (CEO, 0.03–0.48% *v*/*w*), and loaded with bacterial cellulose nanocrystals (BCNCs, 0.06% *w*/*w*) at pH = 3.5. CEO-GelA/BCNC films were prepared by casting, and thickness, light transmittance (TT) and haze (H), surface hydrophobicity, tensile properties, chemical composition, and water solubility (WS) thereof were assessed. All films displayed outstanding optical properties (TT > 89.4%), with haze slightly exceeding a 3% value only at the highest CEO loading within the nanoemulsion formulation. The CEO plasticizing effect increased the elongation at break (EAB, from 0.84% up to 3.79%) and decreased the tensile strength (TS, from 8.98 MPa down to 1.93 MPa). The FT-IR spectra of films revealed good interaction among nanoemulsion components via hydrogen bonding. The CEO hydrophobic nature negatively impacted the WS (from 52.08% down to 8.48%) of the films. The results of this work confirmed the possibility of producing packaging systems from renewable sources to be potentially used in the form of edible films/coatings for the preservation of water-sensitive food products, both vegan-based (fruits/vegetables) and animal-based (meat/seafood).

Keywords: edible films; essential oils; IR spectroscopy; nanoemulsions; surface properties

Citation: Golmohammadi, A.; Razavi, M.S.; Tahmasebi, M.; Carullo, D.; Farris, S. Cinnamon Essential-Oil-Loaded Fish Gelatin–Cellulose Nanocrystal Films Prepared under Acidic Conditions. *Coatings* **2023**, *13*, 1360. https://doi.org/10.3390/coatings13081360

Academic Editor: María B. Pérez-Gago

Received: 28 June 2023
Revised: 31 July 2023
Accepted: 1 August 2023
Published: 3 August 2023

1. Introduction

The development of edible films and coatings from polymers of renewable origin represents a promising strategy to tackle the unceasing usage of fossil sources for producing packaging materials, thus eventually avoiding unpleasant consequences at the environmental level [1–3]. In this scenario, gelatin has been extensively regarded as a potential replacement for synthetic polymers due to its intrinsic features, namely biodegradability, biocompatibility, and good shielding ability against the penetration of gases, oils, and volatile compounds, as well as of UV light [4,5]. In addition, gelatin is recognized for its excellent film-forming characteristics and adhesiveness [6–8]. Fish gelatin, in particular, has represented a valid choice to meet the requirements set by Kosher and Halal dietary laws [9]. However, it has been pointed out that both moisture sensitivity and poor mechanical properties restrict the use of gelatin as food packaging material only to products with low/medium water activity [10,11].

In an attempt to improve the functional properties of gelatin-based films, researchers have proposed a combination with other compounds that is able to compensate for the inherent drawbacks of gelatin. In this regard, it was shown that the incorporation of essential oils (EOs) in gelatin films had a positive effect on the water vapor barrier properties [2,12–16], besides having well-known antimicrobial activity. For example, the use of cinnamon essential oil (CEO) for the generation of active packaging films and coatings

for fungal growth control on postharvest fruits has recently been proposed [17]. Similarly, cellulose nanocrystals (CNCs) can be successfully used in combination with fish gelatin to yield nanocomposite structures with superior mechanical characteristics [18–23].

Within the field of biopolymer films and coatings, cellulose from bacterial sources has raised a great deal of attention compared to its plant-based counterpart in the last few years due to two main reasons: first, bacterial cellulose (BC) shows a comparatively greater purity owing to the absence of lignin, hemicelluloses, organic compounds, and pectin [24]; second, the higher degree of crystallinity found in BC than in plant cellulose straightforwardly facilitates its hydrolysis to nanocrystals (BCNCs) via a top-down technique, thus boosting processing yields [18,25].

In a previous study [26], the effect of pH (3.5 and 5) on the properties of nanoemulsions from fish gelatin–bacterial cellulose nanocrystals containing cinnamon essential oil (CEO-GelA/BCNCs) was investigated, so as to serve the purpose of acting as natural controlled-release systems in the food sector (e.g., active packaging). To this end, specific parameters such as size, ζ-potential, morphology, and encapsulation efficiency of the achieved nanoemulsions were carefully assessed. It was concluded that the addition of gelatin within the tested formulations granted a full coverage of CEO nanodroplets, already surrounded by a web of BCNCs, which then translated into a greater emulsion stability throughout the investigated storage window (30 days at 42 °C). A more recent study explored the functionality of CEO-GelA/BCNC films, arising from nanoemulsions at pH 5, in terms of optical behavior, surface wettability, gas/vapor screening effect, and mechanical properties [22]. Surprisingly, no effects on film transparency and haze were disclosed when applying CEO of increasing concentration during the main preparation step. On top of this, the barrier properties displayed by the obtained films seemed to shift the target toward the shelf-life extension of fresh products, both in the forms of coating or as the inner layer of the packaging system (i.e., the coating in direct contact with the food). Notwithstanding these interesting results, no information was retrieved as far as the effect of a lower pH on film functionality is concerned, with the latter being of utmost importance to possibly widen the range of targeted applications in the food packaging sector.

Therefore, inspired by such a premise, this study was conceived to perform a deep characterization of cinnamon-based films made of gelatin and cellulose nanocrystals obtained using a previously optimized method [22,26], starting from emulsions at pH 3.5, to be potentially used in the food packaging sector as edible films/coatings for prolonging the validity period of different food product categories. To this purpose, several analyses were executed so as to put under the spotlight the optical (transmittance and haze), wetting, solubility, and mechanical properties of the final films, whereas FT-IR spectroscopy enabled collecting information on the degree of interactions established at the intra-/intermolecular level among single nanoemulsion components.

2. Materials and Methods

2.1. Raw Materials and Chemicals

In this work, we used type A gelatin (200 Bloom), extracted from fish skin, and obtained (GelA, Kosher, and Halal certified) from Weishardt (Graulhet, France). As an active compound, cinnamon (*Cinnamomum zeylanicum*) essential oil (CEO) extracted from bark was used. According to the supplier (Plant Therapy Essential Oils Corporate, Twin Falls, ID, USA), its composition determined by GC-MS is as follows: E-cinnamaldehyde: 70.6%; E-cinnamyl acetate: 5.3%; β-caryophyllene: 5.1%; linalool: 4.2%; eugenol: 3.7%; 1,8-cineole + β-phellandrene: 1.2%. For the BC production, *Komagataeibacter sucrofermentans* DSM 15973 (Leibniz Institute DSMZ-German Collection of Microorganisms and Cell Cultures, Braunschweig, Germany) was used in a static fermentation setup, according to the procedure described elsewhere [27]. Sulfuric acid (99% *v*/*v*), ethanol (96% *v*/*v*), and dialysis tubing cellulose membrane (12 kDa, average flat width: 43 mm) were purchased from Sigma-Aldrich-Merck (Milano, Italy).

2.2. Emulsion and Film Preparation

BCNC aqueous suspensions and Pickering emulsions were prepared according to methods reported in a previous work [26]. In particular, Pickering emulsions were obtained using different amounts of CEO (4.5–72 μL) added to 2.25 g of BCNC suspension (pH 3.5) and applying a first emulsification using a UP200St ultrasonicator (Hielscher, Teltow, Germany) at 40 W for 5 min. Afterward, the BCNCs/CEO emulsion was mixed with a fish gelatin aqueous solution (10% *w*/*w*) to finally obtain CEO-GelA/BCNC emulsions with BCNCs and gelatin concentrations of 0.06% and 3% (*w*/*w*), respectively. Eventually, six samples coded as T1G (0.03% *v*/*w* CEO), T2G (0.06% *v*/*w* CEO), T3G (0.12% *v*/*w* CEO), T4G (0.24% *v*/*w* CEO), T5G (0.36% *v*/*w* CEO), and T6G (0.48% *v*/*w* CEO) were obtained and systematically analyzed.

The preparation of the films took place by spreading 6.5 g of each emulsion (T1G–T6G) into Petri dishes (10 cm in diameter), which were then stored at 23 ± 1 °C and 50 ± 5% RH for 48 h. The films were then peeled off from the Petri dishes and left to rest in a desiccator at 23 ± 1 °C and 0% RH for one week to allow complete removal of water. For comparative purposes, control films were generated from CEO-free systems, namely GelA/BCNC nanoemulsions.

2.3. Film Characterization

2.3.1. Film Thickness

Films' thickness (δ, in μm) was measured by a digital micrometer with a precision of 1 μm (Mitutoyo, QuantuMike, Data output IP65, Serial No. 293-180, Mitutoyo Corp, Kawasaki, Japan), at 10 different random locations, both from the center and the edges of the film.

2.3.2. Optical Properties

The total luminous transmittance (TT, in %) and haze (H, in %) of tested films were spectrophotometrically measured using a Lambda 650 high-performance spectrophotometer mounting a 150 mm diameter integrating sphere (PerkinElmer, Waltham, MA, USA) according to ASTM D1003 standard method [28]. Accordingly, the sample was placed at the entrance port of the sphere so that both diffused and specular transmitted light could be trapped.

2.3.3. Wetting Properties

The wettability properties of the films' surface were assessed by measuring the water contact angle (θ, in °) and using an optical contact angle apparatus (OCA 15 Plus—Data Physics Instruments GmbH, Filderstadt, Germany) supported by a video measuring system with a CCD camera and digitizing adapter. Rectangular strips (5 cm^2) were mounted on a sample holder with parallel clamping jaws that allowed us to flatten the surface of the films. Then, a small droplet (2.0 ± 0.5 μL) of Milli-Q water was dispensed (T = 23 ± 1 °C, RH = 50 ± 5%) according to the sessile drop procedure [29]. The software SCA 20 (Data Physics Instruments GmbH, Filderstadt, Germany) was used for data acquisition and elaboration.

2.3.4. Mechanical Properties

Tensile strength (TS, in MPa), elongation at break (EAB, in %), and elastic modulus (E, in MPa) of film strips (6 cm in length; 2 cm in width) were determined using an Instron Universal Testing Machine (STM-20, Norwood, MA, USA), and following the ASTM D882 standard [30]. The initial separation between clamps fixing the sample and the cross-head speed was equal to 5 cm and 1.0 mm/s, respectively. For each sample, TS and EAB were calculated, as shown in Equations (1) and (2), whereas E was calculated by a software-driven procedure relying on the "secant" method [31].

$$TS = F_{MAX}/A \quad (1)$$

$$EAB = (\Delta L/L_0) \times 100 \quad (2)$$

where F_{MAX} (in N) is the maximum load, A is the cross-sectional area (in mm^2) of the samples, ΔL (in mm) is the elongation (i.e., the difference between the initial and final length of the specimen) of the film before rupture, and L_0 (in mm) is the initial length of the film.

2.3.5. Fourier Transform Infrared (FT-IR) Measurement

FT-IR analysis was carried out using an FT-IR Spectrum100 instrument (Perkin Elmer Inc., Waltham, MA, USA), coupled with an Attenuated Total Reflectance (ATR) accessory. All spectra were collected at a resolution of 4 cm^{-1} over a broad wavenumber range (800–4000 cm^{-1}), with each spectrum resulting from an average of 16 scans. Before each test, a background scan was launched to remove any spectral signal originating from carbon dioxide and moisture.

2.3.6. Water Solubility (WS)

WS of films was evaluated using the method of Yao et al. [32], with slight modifications. First, film specimens (2 × 2 cm^2) were immersed in beakers containing 10 mL of distilled water and kept under gentle stirring (50 rpm) at 25 °C for 24 h. The samples were then filtered using filter paper (Whatman No. 1), which was then placed in a drying oven (mod. UN 30, Memmert GmbH, Schwabach, Germany) at 105 °C for 24 h until achieving a constant mass. The solubility in water of films was determined gravimetrically using an analytical balance (mod. ME204, Mettler Toledo, Novate Milanese, Italy) and calculated as follows (Equation (3)):

$$WS = (W_i - W_j)/Wi \times 100 \quad (3)$$

where W_i is the initial weight of film plus filter (in g), and W_j is the weight of dried sample residue plus filter (in g).

2.4. Statistical Analysis

All the analyses were repeated at least three times unless otherwise specified. The mean values and standard deviations (SD) of the experimental data were calculated. Statistically significant differences among the averages were evaluated using a one-way analysis of variance (ANOVA) and Tukey's test ($p \leq 0.05$) using the Minitab 18 statistical software (Coventry, UK).

3. Results and Discussion

3.1. Thickness Measurement

The mean values of the edible films' thickness are displayed in Table 1. The thickness of the films increased monotonically with the concentration of CEO until reaching a maximum value (~37 μm) for the T4G sample, after which a decrease for the formulations T5G and T6G was observed. An opposite trend was previously reported, inasmuch as no significant differences ($p > 0.05$) in terms of thickness between control film and CEO-based GelA/BCNC films were highlighted [22]. At the same time, the results of this study are supported by previous works, whereby the low chemical affinity between gelatin and CEO could have reduced the intermolecular interactions; at the same time, CEO has been demonstrated to act as a plasticizer [26], thus leading to a less dense network with a high free volume, which can be deemed the cause of thickness increments [14]. Similar results were obtained by Jamróz et al. [33] in a work on the thickening effect of Lavender essential oil when embedded in a film-forming starch/furcellaran/gelatin matrix, and by Kilinic et al. [34], who showed that adding *Origanum onites* L. essential oil into gelatin resulted in a significant increase in the films' thickness.

Table 1. Averaged values of thickness (δ), total transmittance (TT), haze (H), water contact angle (θ), and water solubility (WS) of CEO-GelA/BCNC films, as a function of CEO loading.

Sample	δ (μm)	TT (%)	H (%)	θ (°)	WS (%)
Control	24.20 ± 1.75^{a}	90.55 ± 0.30^{a}	0.92 ± 0.02^{a}	78.26 ± 3.51^{a}	52.08 ± 1.76^{da}
T1G	26.90 ± 3.66^{b}	90.51 ± 0.20^{a}	0.96 ± 0.01^{a}	95.97 ± 4.25^{b}	31.90 ± 0.24^{cb}
T2G	29.66 ± 1.75^{c}	90.46 ± 0.40^{a}	1.01 ± 0.02^{a}	94.25 ± 0.69^{b}	31.37 ± 0.51^{bc}
T3G	31.33 ± 2.06^{d}	90.37 ± 0.60^{a}	1.07 ± 0.03^{a}	97.19 ± 1.65^{b}	30.45 ± 0.38^{bcd}
T4G	36.62 ± 3.06^{e}	90.32 ± 0.50^{a}	1.16 ± 0.02^{a}	98.50 ± 3.64^{b}	29.45 ± 1.11^{bcd}
T5G	32.00 ± 2.39^{f}	90.29 ± 0.80^{a}	2.58 ± 0.03^{b}	97.40 ± 3.19^{b}	29.12 ± 0.63^{cd}
T6G	34.25 ± 1.66^{g}	89.38 ± 0.60^{a}	3.18 ± 0.04^{c}	94.10 ± 0.84^{b}	28.48 ± 0.52^{d}

Different superscript letters within the same column denote statistically significant differences ($p < 0.05$) among the mean values.

3.2. Optical Properties

The behavior of CEO-GelA/BCNC films hit with visible light is here expressed in terms of TT and H values (Table 1). In line with previous findings [22], no statistical differences ($p > 0.05$) were revealed among the samples in terms of total transmittance, which indicates that increasing the CEO concentration did not lead to any significant change in the total transmitted light. In addition, the haze analysis revealed that with increasing CEO loading in the film formulations, the 'see-through' capability of the films did not change significantly from the formulation T1G to T4G. However, a significant, though limited, increase in haze was instead observed for the highest CEO concentrations (0.36% v/w and 0.48% v/w) (Table 1). This could be due to the increased scattering of the incident light due to the CEO droplets in the films [22]. These results are in agreement with the findings of Tongnuanchan et al. [2] and Yao et al. [24], who reported a joint behavior for the fish skin gelatin films incorporated with citrus essential oil and gelatin–chitosan films supplemented with D-limonene, respectively.

However, according to the acceptability threshold of 3% in the haze to grant adequate display of the packaged food [35], it can be said that all the films had acceptable optical properties for potential applications as a food packaging material. This can even be deduced from a visual inspection of the films (Figure 1).

Figure 1. Digital camera images of films generated from nanoemulsions containing the lowest (T1G, panel (**a**)) and the highest (T6G, panel (**b**)) amount of CEO.

3.3. Wetting Properties

Table 1 shows the mean water contact angles formed on the surface of gelatin–cellulose nanocrystal films containing different CEO concentrations. θ has been widely adopted as a diagnostic parameter to discriminate between materials with hydrophobic ($\theta > 65°$) or hydrophilic ($\theta < 65°$) surface features [36,37]. At the same time, in the design and development of engineered surfaces, θ can be advantageously used to monitor any significant change in the surface properties of a given material ensuing from physicochemical treatments. In this work, we expected that the addition of CEO could have somehow led to an increase in the hydrophobic behavior of the CEO-based GelA/BCNC films. Compared to the control films, the addition of CEO to GelA/BCNC systems induced a significant ($p < 0.05$) increase in the θ values, which is ascribable to the intrinsic hydrophobic nature of the essential oil. However, there was not a significant difference among CEO-loaded films, suggesting that the CEO concentration cannot be considered a limiting factor in the hydrophobic behavior of the film surfaces within the investigated range (0.03% v/w–0.48% v/w). Interestingly, similar values of θ when adding CEO to GelA/BCNC systems produced at pH = 5 were detected [22]. Overall, these results are in full agreement with previous findings demonstrating that the incorporation of oregano, mint, and D-limonene essential oils in gelatin/chitosan-based formulations increased the surface hydrophobicity of films thereof [12,13,32].

3.4. Mechanical Properties

As far as the mechanical properties are concerned, it is clear (Table 2) that GelA/BCNC films exhibited higher TS and E compared to CEO-incorporated films, which instead have a higher elongation at rupture. From a practical point of view, these data indicate that pristine gelatin/cellulose nanocrystal films are stiffer and more brittle than the same films added with CEO, whereas the latter are more stretchable, as demonstrated by the higher EAB. The impairment of TS and E, as well as the increase in EAB, pertaining to tested films upon CEO addition linearly correlated (averaged $R^2 = 0.987$) with the increase in thickness for T1G-T4G samples observed in Table 1. The overall behavior of the films tested in this work is well-known in the literature and has been previously reported by other authors. In particular, the addition of CEO (as other plasticizing molecules) increased the free volume of the polymer network, presumably hindering not only gelatin–gelatin intermolecular interactions but also gelatin–BCNC bonds (e.g., hydrogen bonding), which is reflected in the decrease in both TS and E [38–40]. For the same reason, CEO improved film extensibility due to its plasticizing effect that enhanced the mobility of gelatin molecules [5,40]. Similarly, Wu et al. [38] observed that CEO nanoliposomes added to fish gelatin curbed the brittleness of generated films at the expense of lower TS values. Analogous conclusions were drawn by Nunes et al. [41] when incorporating lemon essential oils and green tea extracts in gelatin films. Interestingly, differences (though comparable) values of TS, EAB, and E are reported in the literature for films produced from either fish or bovine/porcine/chicken-based gelatins [2,5,12,42–47]. This difference mainly depends on the variation in the aminoacidic content, which is known to mostly affect the gelatin strength. At the same time, a certain degree of variation has been reported for fish gelatin. In this other case, the temperature of the water where the fish lives explains the different values found in the literature [40,48,49]. For instance, gelatin derived from cold-water fish has lower amino acid content compared to that extracted from warm-water fish [50].

Finally, it must be noted that the superior mechanical properties of CEO-GelA/BCNC films produced at pH = 5 [22] compared to films prepared at pH = 3.5 (this work) can be explained considering the pH effect on the strength of fish gelatin-based films, as thoroughly described in the work of Etxabide et al. [51]. More specifically, at a pH = 3.5 pH, the net positive charge is much higher than at pH = 5, which would then promote a more intense electrostatic repulsion at the intermolecular level.

Table 2. Averaged values of tensile strength (TS), elongation at break (EAB), and elastic modulus (E) of CEO-GelA/BCNC films as a function of the CEO loading.

Sample	TS (MPa)	EAB (%)	E (MPa)
Control	8.98 ± 0.31 ^{a}	0.84 ± 0.13 ^{a}	316.03 ± 10.70 ^{a}
T1G	7.78 ± 0.54 ^{ab}	0.93 ± 0.05 ^{a}	307.73 ± 12.03 ^{a}
T2G	7.29 ± 0.37 ^{b}	1.10 ± 0.13 ^{ab}	297.22 ± 13.15 ^{ab}
T3G	6.64 ± 0.74 ^{b}	1.21 ± 0.32 ^{ab}	284.70 ± 20.86 ^{ab}
T4G	4.42 ± 0.58 ^{c}	1.75 ± 0.30 ^{b}	254.75 ± 18.76 ^{ab}
T5G	2.56 ± 0.83 ^{d}	2.90 ± 0.34 ^{c}	226.95 ± 57.03 ^{ac}
T6G	1.93 ± 0.20 ^{d}	3.79 ± 0.47 ^{d}	220.29 ± 27.22 ^{c}

For each investigated parameter, different superscript letters within the same column denote statistically significant differences ($p < 0.05$) among the mean values.

3.5. FTIR Measurements

The FTIR spectra of neat fish gelatin, BCNCs, and CEO-based films thereof provided important insights into the occurrence of intermolecular interactions among the individual components (Figure 2). At a first glance, the CEO-GelA/BCNC spectrum reveals the characteristic fingerprint of the CEO dominated by several peaks within the 1800–600 cm^{-1} range. According to Jeyaratnama et al. [52], the peak at 1566 cm^{-1} corresponds to the C=C skeletal vibration of the aromatic ring of CEO, whereas the peak at 1434 cm^{-1} is assigned to the vibrational absorption of C–OH moieties. The peak at 1324 cm^{-1} is attributed to $–CH_2$ swing in alkanes and =C–H in-plane bending absorption of the aromatic ring, with the symmetric expansion of C–O–C of aromatic acid ester and vibrational stretching of C–OH groups of phenolic components being assigned to the absorbance at 1244 cm^{-1}. In addition, the peak at 746 cm^{-1} involves the vibrational absorption of =C–H in the benzene ring and, ultimately, the peak at 692 cm^{-1} is attributed to the alkenes' vibration absorption. The clear observation of the above peaks suggests that CEO was properly embedded in the main polymer phase, that is, GelA/BCNC emulsion, upon film preparation.

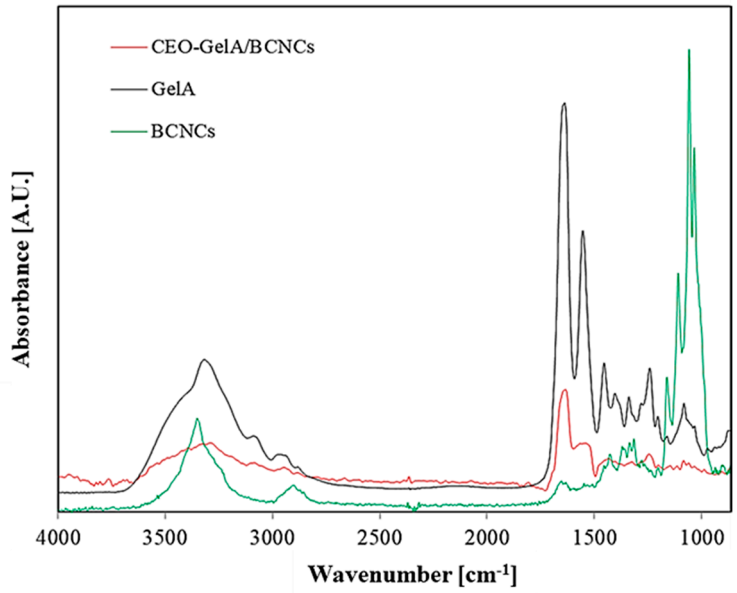

Figure 2. FT-IR spectra of CEO-GelA/BCNC films, neat GelA, and BCNCs. Each spectrum is plotted as a function of the wavenumber (cm^{-1}).

The characteristic peak of gelatin at 3316 cm^{-1} (amide A) is associated with the N-H stretching coupled with hydrogen bonding, while the peak centered at 3089 cm^{-1} (amide B) is assigned to the C-H stretching vibrations. In the amide I/III region (1650–1200 cm^{-1}), the peak at 1638 cm^{-1} is related to the gelatin coil structure and is due to the C=O stretching vibration/hydrogen bonding coupled with COO^{-} groups. The peaks at 1554 cm^{-1} and

1242 cm^{-1} are caused by bending and in-plane vibration of C-N/N-H groups of bound amides, respectively [14,53–59].

Concerning the BCNC spectrum (Figure 2), the peak located at around 3350 cm^{-1} (υ(OH) stretching vibrations) indicates that hydroxyl groups in BCNCs contributed to the formation of different types of inter- and intramolecular hydrogen bonds [60,61], whereas the peaks at 1316, 1162, and 1110 cm^{-1} are prerogatives of the crystalline cellulose (ωs(CH_2) bending vibration), asymmetrical stretching of C–O–C glycosidic bonds, and stretching vibration of C–O, respectively [62]. At last, the small peaks at 1058 and 1035 cm^{-1} are due to the C–O stretching vibrations of the aliphatic primary and secondary alcohols of cellulose [63].

The addition of CEO within the GelA/BCNC formulation caused both subtle shifts in wavenumbers as well as broadening/narrowing of the characteristic peaks of the main polymers. This is clear evidence of the interactions that occurred between the characteristic groups of BCNCs and gelatin, thus indicating good molecular compatibility [23] and possible conformational changes ensuing from these interactions [64–66].

3.6. WS Measurements

The water solubility values of GelA/BCNC films, added or not with CEO, are summarized in Table 1. The addition of the CEO remarkably led to a decrease in WS compared to the GelA/BCNC formulation. In addition, the WS evolution was in an inverse relationship with the concentration of CEO, with a minimum value reached with the T6G sample (0.48% *v*/*w* CEO). This effect has to be ascribed to the increased hydrophobicity of films upon CEO addition, which eventually yielded a lower water solubility. To date, different authors have investigated the influence of essential oils on the solubility of biopolymeric films in aqueous media. Nunes et al. [41] reported that adding a lemon nanoemulsion and green tea extract into gelatin films caused an increase in the water solubility, which was attributed to the establishment of interactions between the hydrophobic groups of oil and tea extract with those distributed along the gelatin chains. Gomez-Estaca et al. [67] and Kavoosi et al. [68] demonstrated that gelatin susceptibility to water solubilization dramatically improved upon clove essential oil and thyme nanoemulsion addition, respectively. Conversely, in full agreement with our results, Jamróz et al. [33] and Kilinic et al. [34] highlighted a great decrease in film water solubility after Lavender and *Origanum onites* L. essential oils were added to gelatin films.

4. Conclusions

This work sheds light on the functional (e.g., optical, surface, and mechanical) and structural properties of CEO-GelA/BCNC edible films obtained from nanoemulsions prepared at a low pH level, that is, 3.5. In particular, despite the thickness increase following the CEO incorporation, the total transmittance of the films was not impaired, whereas a significant increase in haze was observed only for the highest CEO concentration. CEO allowed increasing the overall hydrophobic behavior of the films, thus reflecting the high repellency of the surface toward water and the low degree of solubility in water observed. Finally, the addition of CEO reduced the inherent brittleness of Gel-A/BCNC films, hence making them more suitable for potential food packaging applications. Pending future assessment of the CEO release profile associated with designed films, the outcome of this work suggests their utilization as films/coatings for those applications requiring a slowdown of the water loss process while keeping mechanical integrity and adequate display of the product (e.g., fruits/vegetables, but also meat and seafood products).

Author Contributions: Conceptualization, M.S.R., A.G. and S.F.; methodology, M.S.R., A.G. and S.F.; formal analysis, M.S.R., M.T. and S.F.; investigation, M.S.R., A.G., D.C. and S.F.; data curation, M.S.R. and S.F.; writing—original draft preparation, M.S.R.; writing—review and editing, A.G., M.T., D.C. and S.F.; visualization, M.S.R., D.C. and S.F.; supervision, A.G. and S.F.; project administration, A.G. and S.F.; funding acquisition, A.G. and S.F. All authors have read and agreed to the published version of the manuscript.

Funding: This research received no external funding.

Institutional Review Board Statement: Not applicable.

Informed Consent Statement: Not applicable.

Data Availability Statement: Data are contained within the article.

Acknowledgments: A.G., M.R.S. and M.T. are grateful to the Ministry of Science, Research and Technology of Iran and the University of Mohaghegh Ardabili, for financial support of this project. D.C. and S.F. wish to acknowledge the project "One Health Action Hub: University Task Force for the resilience of territorial ecosystems" supported by Università degli Studi di Milano, PSR 2021. GSA, Linea 6.

Conflicts of Interest: The authors declare no conflict of interest.

References

1. Avena-Bustillos, R.; Chiou, B.S.; Olsen, C.; Bechtel, P.; Olson, D.; McHugh, T. Gelation, oxygen permeability, and mechanical properties of mammalian and fish gelatin films. *J. Food Sci.* **2011**, *76*, E519–E524. [CrossRef] [PubMed]
2. Tongnuanchan, P.; Benjakul, S.; Prodpran, T. Properties and antioxidant activity of fish skin gelatin film incorporated with citrus essential oils. *Food Chem.* **2012**, *134*, 1571–1579. [CrossRef] [PubMed]
3. Echegaray, M.; Mondragon, G.; Loli, M.; González, A.; Peña-Rodriguez, C.; Arbelaiz, A. Physicochemical and mechanical properties of gelatin reinforced with nanocellulose and montmorillonite. *J. Renew. Mater.* **2016**, *4*, 206. [CrossRef]
4. Kanmani, P.; Rhim, J.-W. Physical, mechanical and antimicrobial properties of gelatin based active nanocomposite films containing AgNPs and nanoclay. *Food Hydrocoll.* **2014**, *35*, 644–652. [CrossRef]
5. Tongnuanchan, P.; Benjakul, S.; Prodpran, T.; Pisuchpen, S.; Osako, K. Mechanical, thermal and heat sealing properties of fish skin gelatin film containing palm oil and basil essential oil with different surfactants. *Food Hydrocoll.* **2016**, *56*, 93–107. [CrossRef]
6. Martucci, J.F.; Ruseckaite, R.A. Biodegradation of three-layer laminate films based on gelatin under indoor soil conditions. *Polym. Degrad. Stab.* **2009**, *94*, 1307–1313. [CrossRef]
7. Mu, C.; Guo, J.; Li, X.; Lin, W.; Li, D. Preparation and properties of dialdehyde carboxymethyl cellulose crosslinked gelatin edible films. *Food Hydrocoll.* **2012**, *27*, 22–29. [CrossRef]
8. Peña, C.; Mondragon, G.; Algar, I.; Mondragon, I.; Martucci, J.; Ruseckaite, R. Gelatin films: Renewable resource for food packaging. In *Gelatin: Production, Applications and Health Implications*; Nova Science Publishers: New York, NY, USA, 2013; pp. 1–15.
9. Regenstein, J.; Chaudry, M. Kosher and halal issues pertaining to edible films and coatings. In *Protein-Based Films and Coatings*; Gennadios, A., Ed.; CRC Press: New York, NY, USA, 2002; pp. 601–620.
10. Pérez-Gago, M.B.; Krochta, J. Protein-based films and coatings. In *Edible Coatings and Films to Improve Food Quality*; CRC Press: Boca Raton, FL, USA, 2012; pp. 13–77.
11. Hosseini, S.F.; Rezaei, M.; Zandi, M.; Ghavi, F.F. Preparation and functional properties of fish gelatin–chitosan blend edible films. *Food Chem.* **2013**, *136*, 1490–1495. [CrossRef]
12. Hosseini, S.F.; Rezaei, M.; Zandi, M.; Farahmandghavi, F. Development of bioactive fish gelatin/chitosan nanoparticles composite films with antimicrobial properties. *Food Chem.* **2016**, *194*, 1266–1274. [CrossRef]
13. Scartazzini, L.; Tosati, J.; Cortez, D.; Rossi, M.; Flôres, S.; Hubinger, M.; Di Luccio, M.; Monteiro, A. Gelatin edible coatings with mint essential oil (*Mentha arvensis*): Film characterization and antifungal properties. *J. Food Sci. Technol.* **2019**, *56*, 4045–4056. [CrossRef]
14. Wu, J.; Sun, X.; Guo, X.; Ge, S.; Zhang, Q. Physicochemical properties, antimicrobial activity and oil release of fish gelatin films incorporated with cinnamon essential oil. *Aquac. Fish.* **2017**, *2*, 185–192. [CrossRef]
15. Rashidi, M.J.; Nasiraie, L.R.; Zomorrodi, S.; Jafarian, S. Development and characterization of novel active opopanax gum and gelatin bio-nanocomposite film containing zinc oxide nanoparticles and peppermint essential oil. *J. Food Meas. Charact.* **2023**, *17*, 1953–1961. [CrossRef]
16. Moghadam, F.A.M.; Khoshkalampour, A.; Moghadam, F.A.M.; PourvatanDoust, S.; Naeijian, F.; Ghorbani, M. Preparation and physicochemical evaluation of casein/basil seed gum film integrated with guar gum/gelatin based nanogel containing lemon peel essential oil for active food packaging application. *Int. J. Biol. Macromol.* **2023**, *224*, 786–796. [CrossRef]
17. Sadat Razavi, M.; Golmohammadi, A.; Nematollahzadeh, A.; Ghanbari, A.; Davari, M.; Carullo, D.; Farris, S. Production of Innovative essential oil-based emulsion coatings for fungal growth control on postharvest fruits. *Foods* **2022**, *11*, 1602. [CrossRef] [PubMed]
18. George, J.; Hatna, S. High performance edible nanocomposite films containing bacterial cellulose nanocrystals. *Carbohydr. Polym.* **2012**, *87*, 2031–2037. [CrossRef]
19. Dehnad, D.; Emam-Djomeh, Z.; Mirzaei, H.; Jafari, S.-M.; Dadashi, S. Optimization of physical and mechanical properties for chitosan–nanocellulose biocomposites. *Carbohydr. Polym.* **2014**, *105*, 222–228. [CrossRef]

20. Karimi, S.; Dufresne, A.; Tahir, M.P.; Karimi, A.; Abdulkhani, A. Biodegradable starch-based composites: Effect of micro and nanoreinforcements on composite properties. *J. Mater. Sci.* **2014**, *49*, 4513–4521. [CrossRef]
21. Mondragon, G.; Peña-Rodriguez, C.; González, A.; Eceiza, A.; Arbelaiz, A. Bionanocomposites based on gelatin matrix and nanocellulose. *Eur. Polym. J.* **2015**, *62*, 1–9. [CrossRef]
22. Razavi, M.S.; Golmohammadi, A.; Nematollahzadeh, A.; Rovera, C.; Farris, S. Cinnamon essential oil encapsulated into a fish gelatin-bacterial cellulose nanocrystals complex and active films thereof. *Food Biophys.* **2022**, *17*, 38–46. [CrossRef]
23. Taokaew, S.; Seetabhawang, S.; Siripong, P.; Phisalaphong, M. Biosynthesis and characterization of nanocellulose-gelatin films. *Materials* **2013**, *6*, 782–794. [CrossRef]
24. Yao, J.; Chen, S.; Chen, Y.; Wang, B.; Pei, Q.; Wang, H. Macrofibers with high mechanical performance based on aligned bacterial cellulose nanofibers. *ACS Appl. Mater. Interfaces* **2017**, *9*, 20330–20339. [CrossRef]
25. Lin, K.-W.; Lin, H.-Y. Quality characteristics of chinese-style meatball containing bacterial cellulose (Nata). *J. Food Sci.* **2004**, *69*, SNQ107–SNQ111. [CrossRef]
26. Razavi, M.S.; Golmohammadi, A.; Nematollahzadeh, A.; Fiori, F.; Rovera, C.; Farris, S. Preparation of cinnamon essential oil emulsion by bacterial cellulose nanocrystals and fish gelatin. *Food Hydrocoll.* **2020**, *109*, 106111. [CrossRef]
27. Rovera, C.; Ghaani, M.; Santo, N.; Trabattoni, S.; Olsson, R.T.; Romano, D.; Farris, S. Enzymatic hydrolysis in the green production of bacterial cellulose nanocrystals. *ACS Sustain. Chem. Eng.* **2018**, *6*, 7725–7734. [CrossRef]
28. *Designation D 1003-00*; Standard Test Method for Haze and Luminous Transmittance of Transparent Plastics. American Society for Testing and Materials: Philadelphia, PA, USA, 2000.
29. Rovera, C.; Türe, H.; Hedenqvist, M.S.; Farris, S. Water vapor barrier properties of wheat gluten/silica hybrid coatings on paperboard for food packaging applications. *Food Packag. Shelf Life* **2020**, *26*, 100561. [CrossRef]
30. *Designation D 882-18*; Standard Test Method for Tensile Properties of Thin Plastic Sheeting. American Society for Testing and Materials: Philadelphia, PA, USA, 2018.
31. Cozzolino, C.A.; Campanella, G.; Türe, H.; Olsson, R.T.; Farris, S. Microfibrillated cellulose and borax as mechanical, O2-barrier, and surface-modulating agents of pullulan biocomposite coatings on BOPP. *Carbohydr. Polym.* **2016**, *143*, 179–187. [CrossRef] [PubMed]
32. Yao, Y.; Ding, D.; Shao, H.; Peng, Q.; Huang, Y. Antibacterial activity and physical properties of fish gelatin-chitosan edible films supplemented with D-Limonene. *Int. J. Polym. Sci.* **2017**, *2017*, 1837171. [CrossRef]
33. Jamróz, E.; Konieczna-Molenda, A.; Para, A. Ternary potato starch-furcellaran-gelatin film–a new generation of biodegradable foils. *Polimery* **2017**, *62*, 673–679. [CrossRef]
34. Kilinc, D.; Ocak, B.; Özdestan-Ocak, Ö. Preparation, characterization and antioxidant properties of gelatin films incorporated with Origanum onites L. essential oil. *J. Food Meas. Charact.* **2021**, *15*, 795–806. [CrossRef]
35. Unalan, I.U.; Wan, C.; Figiel, Ł.; Olsson, R.T.; Trabattoni, S.; Farris, S. Exceptional oxygen barrier performance of pullulan nanocomposites with ultra-low loading of graphene oxide. *Nanotechnology* **2015**, *26*, 275703. [CrossRef]
36. Su, J.-F.; Huang, Z.; Yuan, X.-Y.; Wang, X.-Y.; Li, M. Structure and properties of carboxymethyl cellulose/soy protein isolate blend edible films crosslinked by Maillard reactions. *Carbohydr. Polym.* **2010**, *79*, 145–153. [CrossRef]
37. Vogler, E.A. Structure and reactivity of water at biomaterial surfaces. *Adv. Colloid Interface Sci.* **1998**, *74*, 69–117. [CrossRef] [PubMed]
38. Wu, J.; Liu, H.; Ge, S.; Wang, S.; Qin, Z.; Chen, L.; Zheng, Q.; Liu, Q.; Zhang, Q. The preparation, characterization, antimicrobial stability and in vitro release evaluation of fish gelatin films incorporated with cinnamon essential oil nanoliposomes. *Food Hydrocoll.* **2015**, *43*, 427–435. [CrossRef]
39. Ramos, M.; Valdés, A.; Beltran, A.; Garrigós, M.C. Gelatin-based films and coatings for food packaging applications. *Coatings* **2016**, *6*, 41. [CrossRef]
40. Said, N.S.; Sarbon, N.M. Physical and mechanical characteristics of gelatin-based films as a potential food packaging material: A review. *Membranes* **2022**, *12*, 442. [CrossRef]
41. Nunes, J.C.; Melo, P.T.S.; Lorevice, M.V.; Aouada, F.A.; de Moura, M.R. Effect of green tea extract on gelatin-based films incorporated with lemon essential oil. *J. Food Sci. Technol.* **2021**, *58*, 1–8. [CrossRef]
42. Arpi, N.; Hardianti, E. Preparation and characterization of biodegradable film based on skin and bone fish gelatin. *IOP Conf. Ser. Earth Environ. Sci.* **2018**, *207*, 012050. [CrossRef]
43. Atmaka, W.; Yudhistira, B.; Putro, M. Characteristic study of chitosan addition in Tilapia (*Oreochromis niloticus*) bone based gelatin film. *IOP Conf. Ser. Earth Environ. Sci.* **2018**, *142*, 012028. [CrossRef]
44. Jiang, M.; Liu, S.; Du, X.; Wang, Y. Physical properties and internal microstructures of films made from catfish skin gelatin and triacetin mixtures. *Food Hydrocoll.* **2010**, *24*, 105–110. [CrossRef]
45. Jridi, M.; Abdelhedi, O.; Salem, A.; Kechaou, H.; Nasri, M.; Menchari, Y. Physicochemical, antioxidant and antibacterial properties of fish gelatin-based edible films enriched with orange peel pectin: Wrapping application. *Food Hydrocoll.* **2020**, *103*, 105688. [CrossRef]
46. Lee, K.-Y.; Lee, J.-H.; Yang, H.-J.; Song, K.B. Characterization of a starfish gelatin film containing vanillin and its application in the packaging of crab stick. *Food Sci. Biotechnol.* **2016**, *25*, 1023–1028. [CrossRef]
47. Suderman, N.; Isa, M.; Sarbon, N. Characterization on the mechanical and physical properties of chicken skin gelatin films in comparison to mammalian gelatin films. *IOP Conf. Ser. Earth Environ. Sci.* **2018**, *440*, 012033. [CrossRef]

48. Sarbon, N.M.; Badii, F.; Howell, N.K. Preparation and characterisation of chicken skin gelatin as an alternative to mammalian gelatin. *Food Hydrocoll.* **2013**, *30*, 143–151. [CrossRef]
49. Nur Hanani, Z.; Roos, Y.; Kerry, J. Fourier transform ınfrared (FTIR) spectroscopic analysis of biodegradable gelatin films immersed in water. In Proceedings of the 11th International Congress on Engineering and Food, ICEF11, Athens, Greece, 22–26 May 2011; Volume 5, pp. 6–9.
50. Ratnasari, I.; Yuwono, S.; Nusyam, H.; Widjanarko, S. Extraction and characterization of gelatin from different fresh water fishes as alternative sources of gelatin. *Int. Food Res. J.* **2013**, *20*.
51. Etxabide, A.; Leceta, I.; Cabezudo, S.; Guerrero, P.; de la Caba, K. Sustainable fish gelatin films: From food processing waste to compost. *ACS Sustain. Chem. Eng.* **2016**, *4*, 4626–4634. [CrossRef]
52. Jeyaratnam, N.; Nour, A.H.; Kanthasamy, R.; Nour, A.H.; Yuvaraj, A.; Akindoyo, J.O. Essential oil from Cinnamomum cassia bark through hydrodistillation and advanced microwave assisted hydrodistillation. *Ind. Crops Prod.* **2016**, *92*, 57–66. [CrossRef]
53. Hanani, Z.N.; Roos, Y.H.; Kerry, J.P. Use and application of gelatin as potential biodegradable packaging materials for food products. *Int. J. Biol. Macromol.* **2014**, *71*, 94–102. [CrossRef]
54. Haghighi, H.; De Leo, R.; Bedin, E.; Pfeifer, F.; Siesler, H.W.; Pulvirenti, A. Comparative analysis of blend and bilayer films based on chitosan and gelatin enriched with LAE (lauroyl arginate ethyl) with antimicrobial activity for food packaging applications. *Food Packag. Shelf Life* **2019**, *19*, 31–39. [CrossRef]
55. Kumari, S.; Rath, P.; Kumar, A.S.H. Chitosan from shrimp shell (*Crangon crangon*) and fish scales (*Labeorohita*): Extraction and characterization Suneeta. *Afr. J. Biotechnol.* **2016**, *15*, 1258–1268.
56. Hoque, M.S.; Benjakul, S.; Prodpran, T. Effect of heat treatment of film-forming solution on the properties of film from cuttlefish (*Sepia pharaonis*) skin gelatin. *J. Food Eng.* **2010**, *96*, 66–73. [CrossRef]
57. Bergo, P.; Sobral, P.J.d.A. Effects of plasticizer on physical properties of pigskin gelatin films. *Food Hydrocoll.* **2007**, *21*, 1285–1289. [CrossRef]
58. Jamili, S.; Sadeghi, H.; Rezayat, M.; Attar, H.; Kaymaram, F. Extraction and evaluation of gelatin from yellow fin tuna (*Thunnus albacares*) skin and prospect as an alternative to mammalian gelatin. *Iran. J. Fish. Sci.* **2019**, *18*, 903–914.
59. Das, M.P.; Suguna, P.; Prasad, K.; Vijaylakshmi, J.; Renuka, M. Extraction and characterization of gelatin: A functional biopolymer. *Int. J. Pharm. Pharm. Sci.* **2017**, *9*, 239. [CrossRef]
60. Chi, K.; Catchmark, J.M. The influences of added polysaccharides on the properties of bacterial crystalline nanocellulose. *Nanoscale* **2017**, *9*, 15144–15158. [CrossRef]
61. Vasconcelos, N.F.; Feitosa, J.P.A.; da Gama, F.M.P.; Morais, J.P.S.; Andrade, F.K.; de Souza, M.D.S.M.; de Freitas Rosa, M. Bacterial cellulose nanocrystals produced under different hydrolysis conditions: Properties and morphological features. *Carbohydr. Polym.* **2017**, *155*, 425–431. [CrossRef] [PubMed]
62. Lima, H.L.S.; Gonçalves, C.; Cerqueira, M.Â.; do Nascimento, E.S.; Gama, M.F.; Rosa, M.F.; Borges, M.d.F.; Pastrana, L.M.; Brígida, A.I.S. Bacterial cellulose nanofiber-based films incorporating gelatin hydrolysate from tilapia skin: Production, characterization and cytotoxicity assessment. *Cellulose* **2018**, *25*, 6011–6029. [CrossRef]
63. Voronova, M.I.; Surov, O.V.; Guseinov, S.S.; Barannikov, V.P.; Zakharov, A.G. Thermal stability of polyvinyl alcohol/nanocrystalline cellulose composites. *Carbohydr. Polym.* **2015**, *130*, 440–447. [CrossRef]
64. Núñez-Flores, R.; Giménez, B.; Fernández-Martín, F.; López-Caballero, M.; Montero, M.; Gómez-Guillén, M. Physical and functional characterization of active fish gelatin films incorporated with lignin. *Food Hydrocoll.* **2013**, *30*, 163–172. [CrossRef]
65. Santos, T.M.; Men de Sá Filho, M.S.; Caceres, C.A.; Rosa, M.F.; Morais, J.P.S.; Pinto, A.M.; Azeredo, H.M. Fish gelatin films as affected by cellulose whiskers and sonication. *Food Hydrocoll.* **2014**, *41*, 113–118. [CrossRef]
66. Cazón, P.; Velazquez, G.; Ramírez, J.A.; Vázquez, M. Polysaccharide-based films and coatings for food packaging: A review. *Food Hydrocoll.* **2017**, *68*, 136–148. [CrossRef]
67. Gómez-Estaca, J.; De Lacey, A.L.; López-Caballero, M.; Gómez-Guillén, M.; Montero, P. Biodegradable gelatin–chitosan films incorporated with essential oils as antimicrobial agents for fish preservation. *Food Microbiol.* **2010**, *27*, 889–896. [CrossRef] [PubMed]
68. Kavoosi, G.; Rahmatollahi, A.; Dadfar, S.M.M.; Purfard, A.M. Effects of essential oil on the water binding capacity, physico-mechanical properties, antioxidant and antibacterial activity of gelatin films. *LWT-Food Sci. Technol.* **2014**, *57*, 556–561. [CrossRef]